

Morphological Evolution of Thermal Plumes in Turbulent Rayleigh-Bénard Convection

Quan Zhou, Chao Sun, and Ke-Qing Xia

Department of Physics, The Chinese University of Hong Kong, Shatin, Hong Kong, China

(Received 1 September 2006; published 12 February 2007)

An experimental study of the morphological evolution of thermal plumes in turbulent thermal convection is presented. Individual sheetlike plumes are extracted and their area, circumference, and “heat content” are found to all exhibit log-normal distributions. As the sheetlike plumes move across the plate they collide and convolute into spiraling swirls. These swirls then spiral away from the plates to become mushroomlike plumes which are accompanied by strong vertical vorticity. The measured profiles of plume numbers and of vertical vorticity quantify the morphological transition of sheetlike plumes to mushroomlike ones and the mixing and merging or clustering of mushroomlike plumes. The fluctuating vorticity is found to have the same exponential distribution and scaling behavior as the fluctuating temperature.

DOI: [10.1103/PhysRevLett.98.074501](https://doi.org/10.1103/PhysRevLett.98.074501)

PACS numbers: 47.27.-i, 05.65.+b, 44.20.+b, 47.32.C-

Turbulent Rayleigh-Bénard convection (RBC) has become a paradigm for many convection phenomena occurring in nature. A prominent feature of convective thermal turbulence is the ubiquity of coherent structures. One such coherent structure is the thermal plume, which is a localized thermal structure having a temperature contrast with the background fluid and generated from the upper and lower thermal boundary layers of the convection cell. Despite extensive studies of the various aspects of this object, our understanding of the nature of plumes remains incomplete. Many visualization studies have shown two different morphologies for plumes, when observed from above they appear to be sheetlike [1–7] and when viewed from the side they look mushroomlike [2,8–11]. It is generally assumed that as the sheetlike plumes move away from the boundary layer region they morph into mushroomlike ones [7,12]. Because it takes place over a very short distance from the boundary layer, exactly how this transformation came about remains unclear. In addition, the properties of individual plumes, sheetlike or mushroomlike, are poorly understood. Several studies have attempted to characterize or extract plume properties based on local temperature and/or velocity measurements [13–15]. As plumes are geometrical objects, in addition to being a thermal one, results obtained from single point measurement are inevitably incomplete. Because coherent structures, such as plumes in thermal turbulence, play an important role in turbulent flows, their statistical characterization is essential to the understanding of the related phenomena.

This Letter reports an experimental investigation of the statistical properties of extracted individual sheetlike plumes based on both their geometrical and temperature information and the morphological change of sheetlike to mushroomlike plumes. The experiment was conducted in a cylindrical convection cell filled with water. The top and bottom plates of the cell [16] are made of 5 mm thick sapphire discs and its height and internal radius are $H = 18.5$ cm and $r = 9.25$ cm, so the aspect ratio is unity.

Thermochromic liquid crystal (TLC) microspheres (R29C4W from Hallcrest) were used to visualize the temperature field in horizontal fluid layers at varying depth (z) from the top plate. The use of these particles in RBC have been well documented [2,3,10]. The particles used in the present study have a mean diameter of $50 \mu\text{m}$ and density of $1.03\text{--}1.05 \text{ g/cm}^3$, and were suspended in the convecting fluid in very low concentrations (0.01 wt.%). The peak wavelength of their scattered light changes within a temperature window divided as follows: $29^\circ\text{--}29.5^\circ$ for red, $29.5^\circ\text{--}29.7^\circ$ for green, and $29.7^\circ\text{--}33^\circ$ for blue. A 3-mm-thick horizontal sheet of white light, generated by a halogen lamp, passed through the cell parallel to the top plate. A digital camera was used to take streak photographs of the TLC microspheres at a resolution of 2000×1312 pixels and 24 bit dynamic range. With short camera exposure time the photographs give the instantaneous temperature field, and with long exposure time they will in addition show the trajectories of the particles.

Figure 1 shows photographs of the TLC microspheres, taken at the Rayleigh number $\text{Ra} = 2.0 \times 10^9$ and at the Prandtl number $\text{Pr} = 5.4$. At this Ra the thermal boundary layer thickness $\delta_{\text{th}} = 1$ mm [17], and the temperatures of the top and bottom plates are 23.5° and 36.5° , respectively, so the background fluid with mean bulk temperature as well as hot plumes all appear blue, while the cold plumes appear red and green. Note that the 13°C temperature difference between the top and bottom is well within the range in which the Boussinesq approximation is considered to hold strictly [18,19]. Figures 1(a)–1(c), taken, respectively, at $z = 2$ mm, 2.0 cm, and 9.3 cm, show three typical morphologies of plumes. Figures 1(d)–1(f), taken at $z = 2$ mm and sequentially at a time interval of 4 s, show how sheetlike plumes evolve into mushroomlike ones. Figures 1(g)–1(i), taken at $z = 2.0$ cm and at time interval of 2 s, provide the connection between (b) and (c) and illustrate how mushroomlike plumes merge and cluster together along opposite sidewalls. We now examine them in turn. In Figs. 1(a) and 1(d)–1(f) we can see structures in

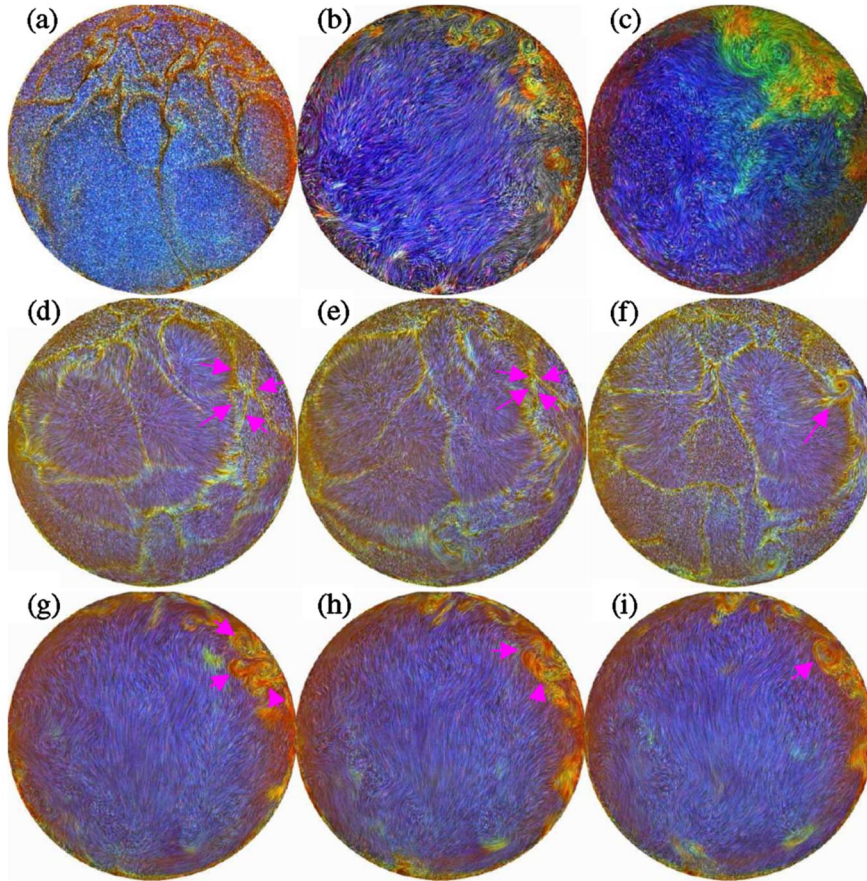


FIG. 1 (color online). Images of TLC microspheres taken at various depth below the top plate: (a) $z = 2$ mm, (b) $z = 2.0$ cm, (c) $z = 9.3$ cm, (d)–(f) same as (a), and (g)–(i) same as (b). The camera exposure time for (a) is 0.02 s, and for (b)–(i) is 0.77 s. In the images cold fluid appears as red and green; hot fluid appears as blue.

the shape of reddish “lines” of finite and varying width and they align mostly in directions perpendicular to the flow. They are very similar to sheetlike plumes observed by others, and will be called as such hereafter. Figure 1(b) shows that most regions with cold temperature (red and green) have intense vortical structures. They are likely to be horizontal cuts of mushroomlike plumes seen in vertical planes of the cell. Both clockwise and anticlockwise swirls are found to be associated with the cold mushroomlike plumes. Plumes associated with vertical vorticity have been found in a numerical study [20], but their connection to sheetlike plumes has not been established. Figures 1(d)–1(f) reveal that where these vortical structures come from, they show that the motion of particles appear to emanate from certain regions or “sources” with bluish color, implying that hot fluid (or hot plumes) are impinging on the top plate from below, then spreading horizontally within the layer and forming waves or sheetlike plumes. Similar features have been observed in previous studies [2,3]. As they move across the plate the particles’ color turns from blue to green and red, suggesting that the wave front is cooled down gradually when spreading. As the sheetlike plumes propagate, they collide with each other or with the sidewall and form swirls [the arrows point to an example of four propagating sheetlike plumes that first collide with each other (d), then merge and convolute (e), and finally form a spiraling swirl (f)]. The vorticity is generated

because the sheetlike plumes carry momenta in different directions before they collide and convolute. For the present Ra , the time scale for the sheetlike plumes to transform into mushroomlike ones varies from 4 to 14 s with a mean of 8 s, while the turnover time of the large-scale circulation (LSC) is 60 s. It is found that over 80% of mushroomlike plumes are formed as a result of the merging and convolution of the sheetlike plumes. Figures 1(g)–1(i) show an example of how plumes merge and cluster. The time scale for the merging and clustering of plumes is found to vary from 2 s to 8 s with a mean of 4 s.

To extract quantitative information of the sheetlike plumes, 200 images were acquired ($z = 2$ mm). The images were acquired at 30 s intervals so that two successive ones are statistically independent. A plume is extracted by first manually drawing a contour around its perimeter and then using a software to collect all pixels enclosed by the contour. To ensure that plumes are identified correctly the operator uses knowledge gained from viewing movies of plume motions. A total of 4001 plumes are identified from the 200 images, which is not a large number but should be indicative of the statistical properties. Figure 2(a) shows an example of extracted plumes with background removed, it corresponds to the image in Fig. 1(a). As each pixel in an image corresponds to a fixed area ($S_{\text{pix}} = 0.16 \times 0.16 \text{ mm}^2$), the area $A_{\text{pl}}^{\text{sheet}}$ and the circumference $C_{\text{pl}}^{\text{sheet}}$ of a plume are readily obtained. To

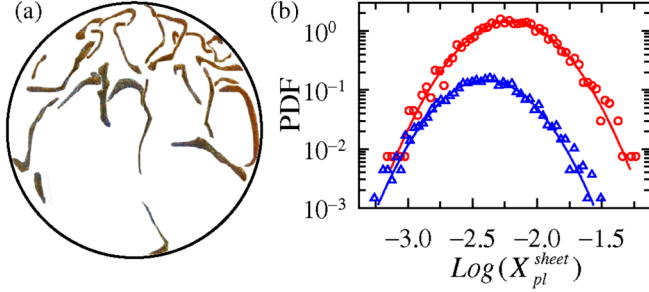


FIG. 2 (color online). (a) An example of extracted sheetlike plumes with background in the original image removed. (b) PDFs of the logarithm of the normalized sheetlike-plume area and heat content, the horizontal axis label $X_{pl}^{sheet} = A_{pl}^{sheet}/\pi r^2$ for circles and Q_{pl}^{sheet}/Q_0 for triangles. For clarity, the vertical scale for $\log(Q_{pl}^{sheet}/Q_0)$ is divided by 10. The curves are Gaussian fittings to the respective data.

obtain temperature distribution among the plumes, the red-green-blue (RGB) signal of each pixel is converted into the hue-saturation-intensity (HSI) color system. The hue is a measure of the peak wavelength in the signal. Using the approximately linear relationship between the hue and the temperature within the narrow sensing window of the TLC particles, the temperature of each pixel is obtained. The “heat” contained in each plume is then calculated as $Q_{pl}^{sheet} = \sum c_p(T_i)\rho(T_i)S_{pix}(T_i - T_0)$, where T_i is the temperature of the i th pixel in a plume, T_0 is the mean temperature of the bulk fluid, c_p and ρ are the specific heat and density of water. Figure 2(b) plots the probability density functions (PDFs) of $\log(A_{pl}^{sheet}/\pi r^2)$ (circles) and $\log(Q_{pl}^{sheet}/Q_0)$ (triangles), which suggest that the area and “heat content” of sheetlike plumes have log-normal distributions. Here Q_0 is the energy supplied to the cell in one large-scale flow turnover time. It is found that C_{pl}^{sheet} also obeys a log-normal distribution. It has been previously found in [13] that, by identifying cliff-ramp structures in temperature time series as thermal plumes, mushroomlike plumes in the cell interior also have log-normal distributions.

The properties of mushroomlike plumes may be obtained by measuring simultaneously the vertical vorticity and the temperature. The vertical component of vorticity $\omega(t)$ was obtained as $\omega = \partial V_y/\partial x - \partial V_x/\partial y$, where the horizontal velocity components $V_x(t)$ and $V_y(t)$ were measured using the particle image velocimetry (PIV) method, the use of which in RBC has been described in [21]. In the present work the local vorticity was measured with a spatial resolution of 1.3 mm. Local temperature $T(t)$ was measured by a thermistor (diameter 0.25 mm) with its tip positioned at a distance of 1.0 ± 0.5 mm from the PIV light sheet. Each measurement lasted 4 hours with a sampling rate of 2 Hz. Three thermistor positions were used [see inset of Fig. 3(a)]. Position A has a vertical distance of 18 mm from the bottom plate and positions B and C are 12 mm from the top plate. The contour in the

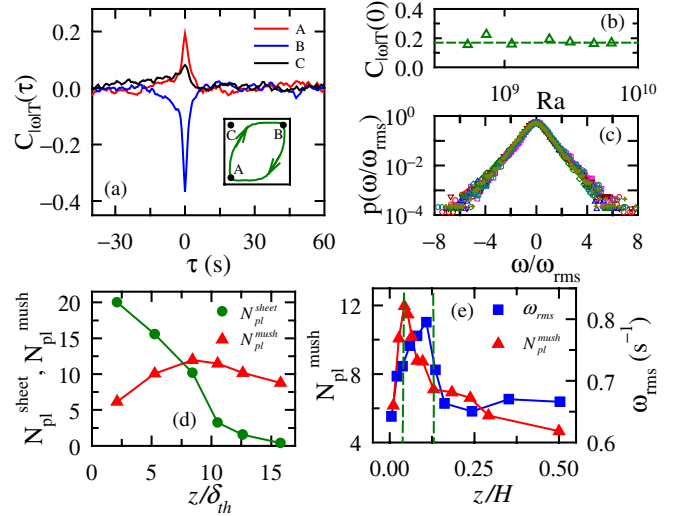


FIG. 3 (color online). (a) Cross-correlation function $C_{|\omega|T}(\tau)$ between vertical vorticity and temperature measured at three positions A, B, and C shown in the inset where the large-scale circulation is also indicated. (b) The correlation amplitude $C_{|\omega|T}(0)$ versus Ra. (c) PDF of normalized vertical vorticity ω/ω_{rms} measured at various Ra from 5.4×10^8 to 6.3×10^9 . (d) Mean numbers of (cold) sheetlike plumes N_{pl}^{sheet} and (cold) mushroomlike ones N_{pl}^{mush} vs the scaled distance z/δ_{th} . (e) Full profiles of N_{pl}^{mush} and of the vorticity fluctuation ω_{rms} vs the scaled distance z/H .

inset indicates the circulation path of the LSC [22], which shows that A and B are near the regions of intense plume emissions [21,23]. The PIV measurement shows that the instantaneous vertical vorticity measured in any horizontal plane is zero when integrated over the horizontal cross section of the cell and that the time-averaged $\omega(t)$ is zero at any position in a horizontal plane. Because both positive and negative vorticity fluctuations are associated with negative temperature fluctuations (for cold plumes), we examine the correlation between $|\omega(t)|$ and $T(t)$. Figure 3(a) shows cross-correlation functions $C_{|\omega|T}(\tau) = \frac{\langle (|\omega(t)| - \langle |\omega| \rangle)(T(t) - \langle T \rangle) \rangle}{\sqrt{\langle (|\omega(t)| - \langle |\omega| \rangle)^2 \rangle \langle (T(t) - \langle T \rangle)^2 \rangle}}$ measured at the three positions (Ra = 3.11×10^9). A positive correlation between T and $|\omega|$ is observed at position A, because the measured T will register a positive spike when hot plumes with temperature higher than the surrounding fluid pass through the thermistor tip. Similar property can be seen at B, where a negative correlation between $|\omega|$ and T is observed due to cold plumes. Mushroomlike plumes are thus concomitant with intense vertical vorticity. We identify swirls with red and green color as cold mushroomlike plumes; i.e., they are defined as objects having nonzero vorticity and having temperatures appreciably lower than that of the background fluid. In contrast, as measured by PIV, laminar plumes produced by point heat source in quiescent fluid have zero vorticity, suggesting that the strong vertical vorticity is associated with the particular way the turbulent plumes are produced, i.e., by the convolution of sheetlike

plumes. When moving upwards or downwards, thermal plumes get stretched and mixed by the velocity field, and their temperature contrast with background fluid also decreases with time. One sees that the magnitude of correlation between $|\omega|$ and T at B is stronger than at A , because B is closer to the boundary layer than A . At C , most hot plumes have been mixed with the background fluid and thus the correlation is even weaker. The simultaneous measurements of ω and T were also made at various values of Ra ranging from 5.4×10^8 to 6.31×10^9 , all at position A . The Ra dependence of ω_{rms} and T_{rms} are found to be very close and may be represented by the power-law fits $\omega_{\text{rms}} = 1.92 \times 10^{-7} Ra^{0.71 \pm 0.02}$ and $T_{\text{rms}} = 1.59 \times 10^{-8} Ra^{0.77 \pm 0.01}$. Also, the cross-correlation amplitude $C_{|\omega|T}(0)$ seems to be independent of Ra [Fig. 3(b)]. The PDF of $\omega/\omega_{\text{rms}}$ in Fig. 3(c) for the 7 values of Ra shows that the vorticity has exponential distribution, which was also found previously [4]. It is well known that temperature PDF in the bulk fluid has exponential distribution [24], while the velocity is Gaussian distributed [23]. Taken together, these results suggest that the fluctuations of vertical vorticity and temperature share similar statistical and scaling properties in places where thermal plumes abound.

The morphological transformation from sheetlike to mushroomlike plumes and the mixing and merging or clustering of plumes may be quantified by the height dependence of their numbers and of vorticity fluctuations. The number of sheetlike plumes $N_{\text{pl}}^{\text{sheet}}$ and that of mushroomlike ones $N_{\text{pl}}^{\text{mush}}$ at various positions [Fig. 3(d)] are obtained by manual counting in each image and then averaging over 100 images for each position. Local vertical vorticities are measured along a vertical line passing through point B ; this is the route most cold plumes traverse downward. Figure 3(e) shows ω_{rms} versus the normalized height z/H , together with the full profile of $N_{\text{pl}}^{\text{mush}}$. It is seen from Figs. 3(d) and 3(e) that mushroomlike plumes increase at the expense of sheetlike ones, which drops quickly from the plate and is essentially zero at $z \approx 15\delta_{\text{th}}$. Also, $N_{\text{pl}}^{\text{sheet}}$ crosses over with $N_{\text{pl}}^{\text{mush}}$ around its peak position at $z \approx 8\delta_{\text{th}}$. The initial rapid increase of ω_{rms} is seen to correspond to the increase of $N_{\text{pl}}^{\text{mush}}$ and the decrease of $N_{\text{pl}}^{\text{sheet}}$, confirming quantitatively the process shown in Fig. 1 that sheetlike plumes merging and convoluting into swirling mushroomlike plumes and thus generating vorticity. The vertical dashed lines in Fig. 3(e) indicate the region of full width at half maximum of ω_{rms} ($z \approx 0.5\text{--}3$ cm). It is seen that in this region of strong vorticity fluctuations $N_{\text{pl}}^{\text{mush}}$ experiences a steep drop, thus providing a quantitative definition and measure of the mixing zone [24] in which most of plume mixing, merging, and clustering take place. It is also interesting to note that the mixing zone found here is roughly the same as that found in [13] based on the skewness of plus and minus temperature increments.

In summary, sheetlike plumes in turbulent thermal convection have been extracted as two-dimensional individual

geometric and thermal objects. The process of sheetlike plumes transform into mushroomlike ones and that of mixing and clustering of plumes have been quantified by the number profiles of the two types of plumes and by the profile of vorticity fluctuations. In addition, it is found that the instantaneous vertical vorticity measured in any horizontal plane is zero when integrated over the horizontal cross section of the cell and that the time-averaged vorticity is zero at any position in a horizontal plane. This work represents the first attempt to quantitatively characterize the morphological change and the geometric properties of these coherent structures, which are largely unexplored. It remains a challenge to extract mushroomlike plumes as three-dimensional objects.

We thank J. Zhang for useful comment on the preprint. This work was supported by the Hong Kong Research Grants Council (Grant No. CUHK403705) and a CUHK Direct Grant (Project No. 4450088). K.Q.X. acknowledges support by the Croucher Foundation of Hong Kong.

-
- [1] H. Tanaka and H. Miyata, *Int. J. Heat Mass Transfer* **23**, 1273 (1980).
 - [2] G. Zocchi, E. Moses, and A. Libchaber, *Physica (Amsterdam)* **A166**, 387 (1990).
 - [3] B.J. Gluckman, H. Willaime, and J.P. Gollub, *Phys. Fluids A* **5**, 647 (1993).
 - [4] P. Vorobie and R. Ecke, *J. Fluid Mech.* **458**, 191 (2002).
 - [5] D. Funfschilling and G. Ahlers, *Phys. Rev. Lett.* **92**, 194502 (2004).
 - [6] T. Haramina and A. Tilgner, *Phys. Rev. E* **69**, 056306 (2004).
 - [7] B. A. Puthenveetil and J. H. Arakeri, *J. Fluid Mech.* **542**, 217 (2005).
 - [8] E. Moses *et al.*, *Europhys. Lett.* **14**, 55 (1991).
 - [9] J. Zhang, S. Childress, and A. Libchaber, *Phys. Fluids* **9**, 1034 (1997).
 - [10] Y.-B. Du and P. Tong, *Phys. Rev. Lett.* **81**, 987 (1998).
 - [11] H.-D. Xi, S. Lam, and K.-Q. Xia, *J. Fluid Mech.* **503**, 47 (2004).
 - [12] A. Parodi *et al.*, *Phys. Rev. Lett.* **92**, 194503 (2004).
 - [13] S.-Q. Zhou and K.-Q. Xia, *Phys. Rev. Lett.* **89**, 184502 (2002).
 - [14] E. S. C. Ching *et al.*, *Phys. Rev. Lett.* **93**, 124501 (2004).
 - [15] A. Bershadskii *et al.*, *Phys. Rev. E* **69**, 056314 (2004).
 - [16] H.-D. Xi, Q. Zhou, and K.-Q. Xia, *Phys. Rev. E* **73**, 056312 (2006).
 - [17] S.-L. Lui and K.-Q. Xia, *Phys. Rev. E* **57**, 5494 (1998).
 - [18] D. Funfschilling *et al.*, *J. Fluid Mech.* **536**, 145 (2005).
 - [19] C. Sun *et al.*, *J. Fluid Mech.* **542**, 165 (2005).
 - [20] T. Cortese and S. Balachandar, *Phys. Fluids A* **5**, 3226 (1993).
 - [21] C. Sun, K.-Q. Xia, and P. Tong, *Phys. Rev. E* **72**, 026302 (2005).
 - [22] C. Sun and K.-Q. Xia, *Phys. Rev. E* **72**, 067302 (2005).
 - [23] X.-L. Qiu and P. Tong, *Phys. Rev. E* **64**, 036304 (2001).
 - [24] B. Castaing *et al.*, *J. Fluid Mech.* **204**, 1 (1989).